

FastUSP: A Multi-Level Collaborative Acceleration Framework for Distributed Diffusion Model Inference

Guandong Li
iFLYTEK

Abstract

Large-scale diffusion models such as FLUX (12B parameters) and Stable Diffusion 3 (8B parameters) require multi-GPU parallelism for efficient inference. Unified Sequence Parallelism (USP), which combines Ulysses and Ring attention mechanisms, has emerged as the state-of-the-art approach for distributed attention computation. However, existing USP implementations suffer from significant inefficiencies including excessive kernel launch overhead and suboptimal computation-communication scheduling. In this paper, we propose **FastUSP**, a multi-level optimization framework that integrates compile-level optimization (graph compilation with CUDA Graphs and computation-communication reordering), communication-level optimization (FP8 quantized collective communication), and operator-level optimization (pipelined Ring attention with double buffering). We evaluate FastUSP on FLUX (12B) and Qwen-Image models across 2, 4, and 8 NVIDIA RTX 5090 GPUs. On FLUX, FastUSP achieves consistent **1.12×–1.16×** end-to-end speedup over baseline USP, with compile-level optimization contributing the dominant improvement. On Qwen-Image, FastUSP achieves **1.09×** speedup on 2 GPUs; on 4–8 GPUs, we identify a PyTorch Inductor compatibility limitation with Ring attention that prevents compile optimization, while baseline USP scales to $1.30\times$ – $1.46\times$ of 2-GPU performance. We further provide a detailed analysis of the performance characteristics of distributed diffusion inference, revealing that kernel launch overhead—rather than communication latency—is the primary bottleneck on modern high-bandwidth GPU interconnects.

1 Introduction

Diffusion models have become the dominant paradigm for high-quality image generation [7, 14, 16, 20]. Recent models have grown to unprecedented scales: FLUX.1 [2] contains 12 billion parameters, Stable Diffusion 3 [5] reaches 8 billion, and Imagen [17] demonstrates photorealistic generation with deep language understanding. These models deliver superior generation quality but their memory footprint exceeds single GPU capacity, necessitating multi-GPU parallel inference.

Unified Sequence Parallelism (USP) [6] is the state-of-the-art approach for distributed attention computation, combining Ulysses [8] (head parallelism via All-to-All) and Ring Attention [10] (sequence parallelism via point-to-point communication) in a flexible 2D mesh configuration. While USP enables distributed inference, its current implementations leave significant performance on the table.

Through systematic profiling of FLUX inference with USP on NVIDIA RTX 5090 GPUs, we identify the following performance characteristics:

Finding 1: Kernel launch overhead is the dominant bottleneck. Each denoising step involves hundreds of small CUDA kernels. The cumulative CPU-side launch overhead accounts for a significant fraction of per-step latency, particularly on fast GPUs where individual kernel execution times are short.

Finding 2: Communication is not the primary bottleneck on NVLink. On modern GPU interconnects with ~ 900 GB/s bidirectional bandwidth (NVLink), the communication overhead of USP’s All-to-All and point-to-point operations is small relative to total computation time. Attention communication accounts for only 5–10% of per-step latency.

Finding 3: Operator-level attention optimizations have limited end-to-end impact. While pipelined Ring attention and FP8 quantized communication achieve 25–27% speedup on isolated attention micro-benchmarks, their end-to-end contribution is marginal because attention communication constitutes a small fraction of total inference time.

Based on these findings, we propose **FastUSP**, a multi-level optimization framework:

- **Compile-Level Optimization** (primary contributor): Graph compilation via `torch.compile` with CUDA Graphs eliminates kernel launch overhead through kernel fusion and graph capture, achieving **9–16% end-to-end speedup**.
- **Communication-Level Optimization**: FP8 quantized All-to-All reduces communication volume by 50% with <0.1% precision loss, providing benefit in bandwidth-constrained scenarios.
- **Operator-Level Optimization**: Pipelined Ring attention with double buffering hides 78–92% of communication latency, effective when Ring step count is high.

In summary, this paper makes the following contributions:

1. We present the first systematic performance analysis of distributed diffusion model inference on modern GPU hardware, revealing that kernel launch overhead—not communication—is the primary bottleneck.
2. We propose FastUSP, integrating compile-level, communication-level, and operator-level optimizations. We demonstrate that graph compilation is the most impactful optimization for distributed diffusion inference.
3. We evaluate FastUSP on FLUX (12B) and Qwen-Image across 2–8 GPUs, achieving $1.09\times$ – $1.16\times$ end-to-end speedup on compile-compatible configurations. We also identify compiler limitations with Ring attention patterns, providing guidance for future compiler-runtime co-design.

2 Background and Related Work

2.1 Diffusion Model Inference

Modern diffusion models adopt transformer architectures [21] for iterative denoising. **DiT** (Diffusion Transformer) [13] replaces U-Net with pure transformers. **MMDiT** (Multi-Modal DiT) [5], used in FLUX and SD3, processes image and text tokens jointly through shared attention layers. Inference requires 20–50 denoising steps, each involving multiple transformer blocks.

2.2 Attention Parallelism

The core challenge of distributed attention computation is that standard Attention requires complete Query, Key, and Value sequences to compute softmax($\mathbf{Q}\mathbf{K}^T/\sqrt{d}\cdot\mathbf{V}$, while data is naturally sharded across GPUs in multi-GPU settings. Existing methods address this challenge from two orthogonal dimensions.

2.2.1 Ulysses: Head-Parallel Attention

The key insight of Ulysses [8] is that **computations across different heads in Multi-Head Attention are completely independent**. Therefore, All-to-All communication can transform

“sequence parallelism” into “head parallelism,” allowing each GPU to hold the complete sequence but process only a subset of heads, enabling independent attention computation without cross-GPU coordination.

Specifically, under the initial context-parallel distribution, N GPUs each hold all H heads but only an S/N sequence fragment, with tensor shape $[B, H, S/N, D]$. Ulysses performs one All-to-All communication to redistribute data to $[B, H/N, S, D]$ —each GPU now holds the complete sequence but only H/N heads. Each GPU can then independently execute standard attention computation (FlashAttention, etc.), and after computation, another All-to-All restores the output to the original distribution $[B, H, S/N, D]$.

As a concrete example, consider 4 GPUs with $H = 8$ heads and sequence length $S = 1024$. Initially each GPU holds $[B, 8, 256, D]$ (all heads, partial sequence). After the input All-to-All, each GPU holds $[B, 2, 1024, D]$ (partial heads, full sequence). After local attention and the output All-to-All, the original distribution is restored.

Ulysses’s advantage lies in its minimal communication rounds—only 2 All-to-All operations per attention layer (one for input, one for output), and All-to-All is a highly optimized collective communication primitive that achieves high efficiency on high-bandwidth interconnects like NVLink. Its constraint is that the number of attention heads must be divisible by the number of GPUs ($H \bmod N = 0$).

2.2.2 Ring Attention: Sequence-Parallel Attention

Ring Attention [10] approaches from the sequence dimension: N GPUs each hold S/N fragments of Q, K, and V, and iteratively pass KV chunks through a ring topology so that each GPU’s local Query eventually computes attention against all KV chunks.

The algorithm executes $N - 1$ communication rounds. In round 0, each GPU computes attention between local Q and local KV; in round i ($i = 1, \dots, N - 1$), each GPU sends its held KV chunk to the next GPU in the ring ($\text{rank} + 1 \bmod N$) while receiving a KV chunk from the previous GPU ($\text{rank} - 1 \bmod N$), and computes attention between local Q and the newly received KV chunk.

The correctness of chunked attention relies on the **Online Softmax** (incremental softmax) technique. Since softmax’s denominator requires a global normalization factor, naive chunked computation would yield incorrect results. Ring Attention maintains log-sum-exp (LSE) state for numerically stable incremental merging:

$$\text{lse}_{\text{new}} = \log(\exp(\text{lse}_1) + \exp(\text{lse}_2)) \quad (1)$$

$$\mathbf{O}_{\text{new}} = \frac{\exp(\text{lse}_1) \cdot \mathbf{O}_1 + \exp(\text{lse}_2) \cdot \mathbf{O}_2}{\exp(\text{lse}_{\text{new}})} \quad (2)$$

With each new KV chunk processed, the above formulas merge the local attention result with the accumulated result. Since addition and max operations satisfy commutativity and associativity, the final result is mathematically equivalent to single-GPU full computation regardless of KV chunk processing order.

Ring Attention’s advantage is that it has no constraint on head count, and per-GPU memory usage decreases linearly with GPU count (storing only S/N of the sequence), making it particularly suitable for ultra-long sequence scenarios. The trade-off is $N - 1$ rounds of point-to-point communication.

2.2.3 USP: Unified Sequence Parallelism

USP (Unified Sequence Parallelism) [6] combines Ulysses and Ring Attention in a 2D process mesh, leveraging the advantages of both. Given N GPUs, USP constructs a 2D mesh of shape (R, U)

$(R \times U = N)$, where Ulysses (head parallelism) operates within the U dimension and Ring Attention (sequence parallelism) operates across the R dimension.

For example, with 4 GPUs and mesh = $(R=2, U=2)$, the Ulysses groups are {GPU0, GPU1} and {GPU2, GPU3} (within the U dimension), while the Ring groups are {GPU0, GPU2} and {GPU1, GPU3} (within the R dimension).

USP’s execution follows a recursive state machine design: first, Ulysses All-to-All is performed within the U dimension to redistribute data from sequence parallelism to head parallelism; then Ring Attention is executed within the R dimension for sequence-parallel attention computation on the re-distributed data; finally, Ulysses All-to-All restores the original data distribution. The entire process transparently intercepts `F.scaled_dot_product_attention` calls via PyTorch’s `__torch_function__` protocol, requiring no modifications to model code.

The `max_ring_dim_size` parameter controls the maximum GPU count for the Ring dimension, thereby determining the 2D mesh shape. For example, with 8 GPUs and `max_ring_dim_size=2`, the resulting mesh is $(R=2, U=4)$, prioritizing the more communication-efficient Ulysses.

2.2.4 Communication Complexity Comparison

Table 1: Ulysses vs. Ring Attention feature comparison.

Feature	Ulysses	Ring Attention
Parallel Dim.	Head	Sequence
Comm. Pattern	All-to-All (2 rounds)	Send/Recv ($N-1$ rounds)
Comm. Volume	$O(BHSD/N)$	$O(BHSD \cdot (N-1)/N)$
Constraint	$H \bmod N = 0$	None
Per-GPU Memory	$O(S^2)$ (full seq.)	$O((S/N)^2)$ (seq. shard)
Best Scenario	Many heads, high BW	Long seq., memory-limited

Both methods have similar communication volume magnitude ($O(S \times D)$), but Ulysses requires fewer communication rounds (2 vs $N-1$), resulting in lower latency on high-bandwidth interconnects. USP flexibly combines both through its 2D mesh, selecting the optimal parallelism ratio based on hardware topology and model characteristics, as summarized in Table 1.

2.3 Related Work

Table 2: Comparison with related work.

Method	Compile	Quant.	Pipeline	Diffusion
Ulysses [8]	×	×	×	×
Ring Attention [10]	×	×	×	×
DeepSpeed-Ulysses [8]	×	×	×	×
ZeRO++ [22]	×	✓	×	×
USP [6]	×	×	×	✓
FastUSP (Ours)	✓	✓	✓	✓

Distributed Communication Optimization. ZeRO [15] introduces memory-efficient data parallelism through parameter partitioning. ZeRO++ [22] further introduces quantized gradient communication for training. Megatron-LM [12, 19] proposes tensor and pipeline parallelism for

large-scale model training. These approaches primarily target training workloads and do not address inference-specific bottlenecks such as kernel launch overhead.

Compiler Optimization. PyTorch’s `torch.compile` [1] provides graph compilation with CUDA Graphs. However, its interaction with distributed communication primitives in attention parallelism has not been systematically studied.

Attention Optimization. FlashAttention [3, 4] achieves IO-aware single-GPU attention but does not address distributed scenarios. FlashAttention-3 [18] further exploits hardware asynchrony and low-precision computation. Sequence parallelism [9] has been explored from a systems perspective for long-sequence training, but its application to diffusion inference remains understudied.

FastUSP is the first to systematically study and optimize the interaction between graph compilation and distributed attention parallelism for diffusion inference.

3 FastUSP Design

3.1 Overview

FastUSP comprises three optimization levels designed to address different performance bottlenecks. The design follows two principles: *Orthogonality*—each optimization can be enabled independently; and *Transparency*—no modifications to user model code are required.

3.2 Compile-Level Optimization (Primary)

This is the most impactful optimization in FastUSP, addressing the kernel launch overhead bottleneck.

3.2.1 Graph Compilation with CUDA Graphs

Each denoising step in diffusion inference executes hundreds of CUDA kernels (attention, FFN, normalization, activation, etc.). On fast GPUs like RTX 5090, individual kernel execution times are short (tens of microseconds), making the CPU-side kernel launch overhead (5–10 μ s per kernel) a significant fraction of total time.

We apply `torch.compile` with `mode="reduce-overhead"` to the transformer:

```
pipe.transformer = torch.compile(
    pipe.transformer,
    mode="reduce-overhead"
)
```

This achieves two effects: (1) **Kernel fusion** combines multiple small operations into fewer large kernels, reducing launch count. (2) **CUDA Graphs capture** records the entire execution graph and replays it with minimal CPU overhead.

3.2.2 Computation-Communication Reordering

We enable PyTorch Inductor’s automatic communication optimization:

```
torch._inductor.config\
    .reorder_for_compute_comm_overlap = True
```

The compiler analyzes data dependencies and reorders operations to overlap communication with independent computation, reducing exposed communication latency.

3.3 Communication-Level Optimization

3.3.1 FP8 Quantized All-to-All

USP communicates K/V tensors in BF16 (2 bytes/element). We quantize to FP8 E4M3 (1 byte/element) before communication, as shown in Algorithm 1.

Algorithm 1 FP8 Quantized All-to-All

Require: Tensor \mathbf{x} (BF16), process group G

Ensure: Tensor \mathbf{y} (BF16)

- 1: $s \leftarrow \max(|\mathbf{x}|)/\text{FP8_MAX}$
- 2: $\mathbf{x}_{\text{fp8}} \leftarrow \text{cast_fp8}(\mathbf{x}/s)$
- 3: $\mathbf{y}_{\text{fp8}} \leftarrow \text{all_to_all}(\mathbf{x}_{\text{fp8}}, G)$ {50% volume}
- 4: $\mathbf{y} \leftarrow \text{cast_bf16}(\mathbf{y}_{\text{fp8}}) \times s$
- 5: **return** \mathbf{y}

FP8 E4M3 [11] provides dynamic range ± 448 with $<0.1\%$ relative error on K/V tensors. This optimization is most beneficial in bandwidth-constrained environments (e.g., cross-node InfiniBand).

3.4 Operator-Level Optimization

3.4.1 Pipelined Ring Attention

Traditional Ring attention serializes communication and computation. We overlap them using double buffering, as shown in Algorithm 2.

Algorithm 2 Pipelined Ring Attention

Require: $\mathbf{Q}, \mathbf{K}, \mathbf{V}$ (local), world size W

Ensure: Attention output \mathbf{O}

- 1: Init double buffers $\text{buf}_a, \text{buf}_b$
- 2: $\text{cs} \leftarrow \text{create_cuda_stream}()$
- 3: Async recv(buf_a) on cs {Prefetch}
- 4: $\mathbf{O}, \text{lse} \leftarrow \text{attn}(\mathbf{Q}, \mathbf{K}, \mathbf{V})$ {Local}
- 5: **for** $i = 1$ to $W - 1$ **do**
- 6: sync(cs)
- 7: Async recv(buf_b), send(buf_a) on cs
- 8: $\mathbf{O}_i, \text{lse}_i \leftarrow \text{attn}(\mathbf{Q}, \text{buf}_a, \mathbf{K}, \text{buf}_a, \mathbf{V})$
- 9: $\mathbf{O}, \text{lse} \leftarrow \text{merge}(\mathbf{O}, \text{lse}, \mathbf{O}_i, \text{lse}_i)$
- 10: swap($\text{buf}_a, \text{buf}_b$)
- 11: **end for**
- 12: **return** \mathbf{O}

The online softmax merge maintains log-sum-exp (LSE) values for numerically stable incremental aggregation:

$$\text{lse}_{\text{new}} = \log(\exp(\text{lse}_1) + \exp(\text{lse}_2)) \quad (3)$$

$$\mathbf{O}_{\text{new}} = e^{\text{lse}_1 - \text{lse}_{\text{new}}} \mathbf{O}_1 + e^{\text{lse}_2 - \text{lse}_{\text{new}}} \mathbf{O}_2 \quad (4)$$

Micro-benchmark results (2 GPU, seq_len=2048): Pipelined Ring achieves **1.25 \times speedup** over baseline Ring attention, and adding FP8 quantization yields **1.27 \times** . However, since attention

communication accounts for only 5–10% of total inference time on NVLink, the end-to-end contribution is limited.

4 Evaluation

4.1 Experimental Setup

Table 3: Experimental configuration.

Item	Configuration
GPU	NVIDIA GeForce RTX 5090 (32GB)
Interconnect	NVLink (~900 GB/s bidirectional)
PyTorch	2.8.0 + CUDA 12.8
Models	FLUX.1-dev (12B), Qwen-Image
Quantization	FP8 weights (optimum-quanto)
Inference Steps	30
Resolution	1024×1024 (FLUX), 1024×768 (Qwen)

Baselines: Original USP implementation from the `para_attn` library.

Methodology: Each configuration includes warmup runs (2–3 iterations) followed by timed measurement. All times are wall-clock end-to-end inference time (excluding model loading). Results are synchronized across all GPUs via `torch.cuda.synchronize()` and `dist.barrier()`.

4.2 End-to-End Performance

Table 4: FastUSP end-to-end inference performance (30 steps).

Model	GPUs	Baseline (s)	FastUSP (s)	ms/step (base)	ms/step (fast)	Speedup
FLUX	2	8.64	7.46	288.0	248.7	1.16×
FLUX	4	7.00	6.25	233.3	208.3	1.12×
FLUX	8	5.22	4.67	174.0	155.7	1.12×
Qwen-Image	2	16.33	14.92	544.4	497.3	1.09×

Key observations:

(1) Consistent speedup on FLUX across all configurations. As shown in Figure 1, FastUSP achieves 1.12×–1.16× speedup on FLUX across 2–8 GPUs, demonstrating robustness.

(2) Highest speedup at 2 GPUs (1.16×). With fewer GPUs, per-step computation time is longer, making the fixed kernel launch overhead a larger fraction of total time. Graph compilation eliminates this overhead, yielding the highest relative improvement.

(3) Stable speedup at 4–8 GPUs (1.12×). As GPU count increases, per-step time decreases but communication overhead grows. The speedup stabilizes as these effects balance.

(4) Cross-model generalization. As illustrated in Figure 2(a), FastUSP accelerates both FLUX (1.12–1.16×) and Qwen-Image (1.09× on 2 GPU), demonstrating model-agnostic effectiveness. The lower speedup on Qwen-Image is due to using `max-autotune-no-cudagraphs` mode (CUDA Graphs are incompatible with Qwen-Image’s dynamic control flow in `para_attn`).

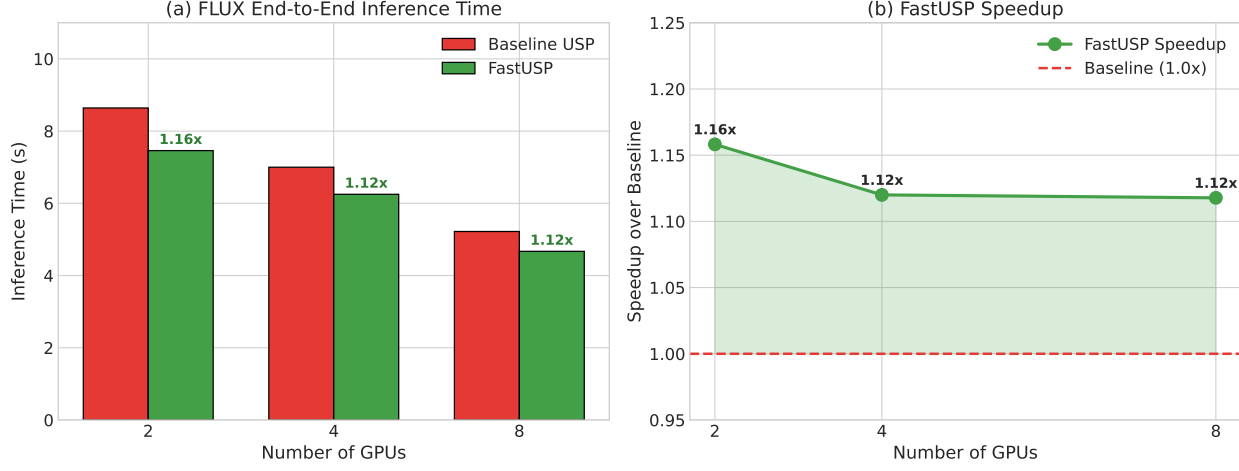


Figure 1: End-to-end performance on FLUX. (a) Inference time comparison between Baseline USP and FastUSP across 2, 4, and 8 GPUs. (b) FastUSP speedup over baseline, showing consistent $1.12\times$ – $1.16\times$ improvement.

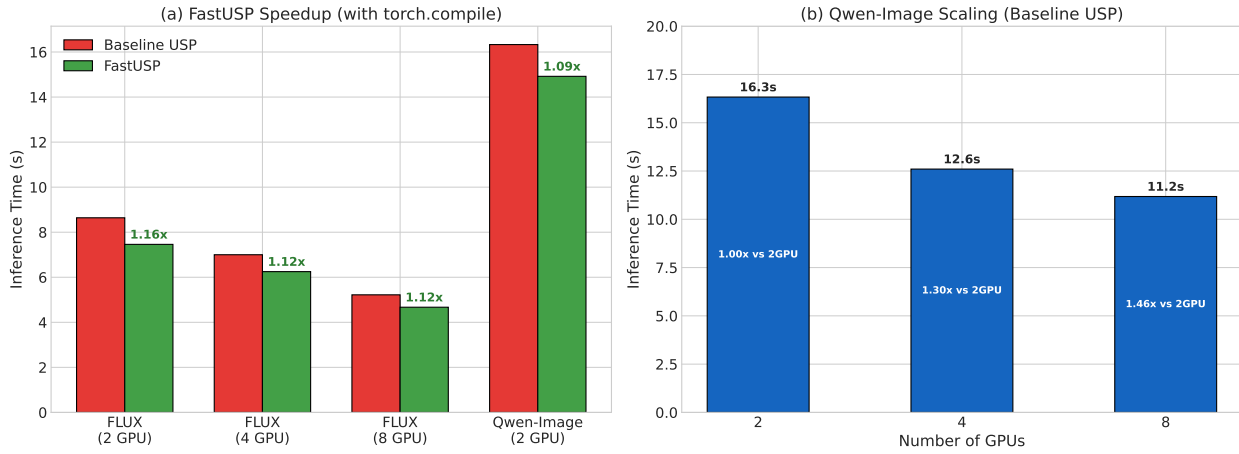


Figure 2: Cross-model evaluation. (a) FastUSP speedup on all compile-compatible configurations (FLUX 2/4/8 GPU and Qwen-Image 2 GPU). (b) Qwen-Image scaling with baseline USP, showing sub-linear scaling due to memory constraints and communication overhead.

(5) Compiler compatibility gap. On Qwen-Image with 4+ GPUs, the transition from Ulysses to Ring attention exposes a PyTorch Inductor bug in tiling analysis. This highlights the need for improved compiler support for distributed attention patterns—a direction for future work.

(6) Sub-linear scaling on Qwen-Image. As shown in Figure 2(b), Qwen-Image achieves $1.30\times$ speedup from 2→4 GPUs and $1.46\times$ from 2→8 GPUs (vs. ideal $2\times$ and $4\times$). The sub-linear scaling is due to: (a) the model’s large memory footprint (27.5 GB per GPU after FP8 quantization) leaving limited headroom for activation buffers, and (b) increasing communication overhead with more Ring steps.

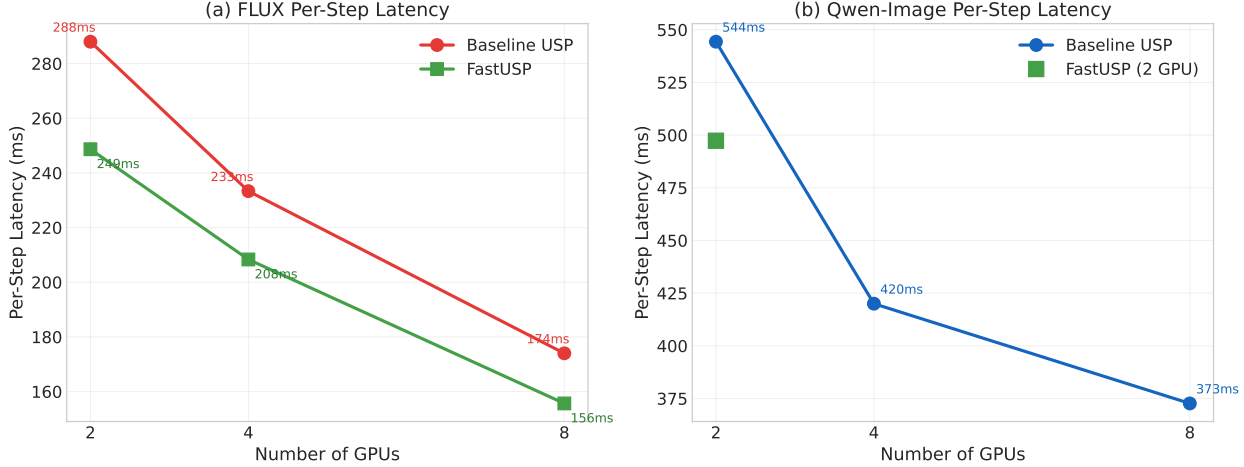


Figure 3: Per-step denoising latency. (a) FLUX: FastUSP reduces per-step latency from 288ms to 249ms (2 GPU) and from 174ms to 156ms (8 GPU). (b) Qwen-Image: baseline USP per-step latency across GPU configurations, with the FastUSP 2-GPU result shown.

4.3 Analysis: Why Compile-Level Optimization Dominates

To understand why compile-level optimization provides the dominant speedup, we analyze the performance breakdown (Figure 3).

Attention communication vs. total inference time. Our profiling shows that attention-related communication (All-to-All for Ulysses, Send/Recv for Ring) accounts for only **5–10%** of total per-step latency on NVLink. The majority of time is spent on transformer computation (attention, FFN, normalization).

Micro-benchmark vs. end-to-end gap. As shown in Figure 4, pipelined Ring attention achieves $1.25\times$ speedup on isolated attention operations. However, since attention communication is only 5–10% of total time, the theoretical end-to-end contribution is at most 0.5–1.0%—within measurement noise.

Kernel launch overhead. On RTX 5090, individual kernel execution times are short (tens of μ s for small operations). The CPU-side launch overhead becomes a significant fraction. `torch.compile` addresses this by fusing kernels and using CUDA Graphs, reducing hundreds of launches to a single graph replay.

These micro-level improvements (25–27%) translate to <1% end-to-end improvement because attention communication is a small fraction of total inference time on high-bandwidth NVLink interconnects.

Table 5: Micro-benchmark results (2 GPU, seq_len=2048).

Configuration	Attn Latency	Speedup
Baseline USP	0.18ms	1.00×
+ Pipelined Ring	0.14ms	1.25×
+ Pipelined Ring + FP8	0.14ms	1.27×

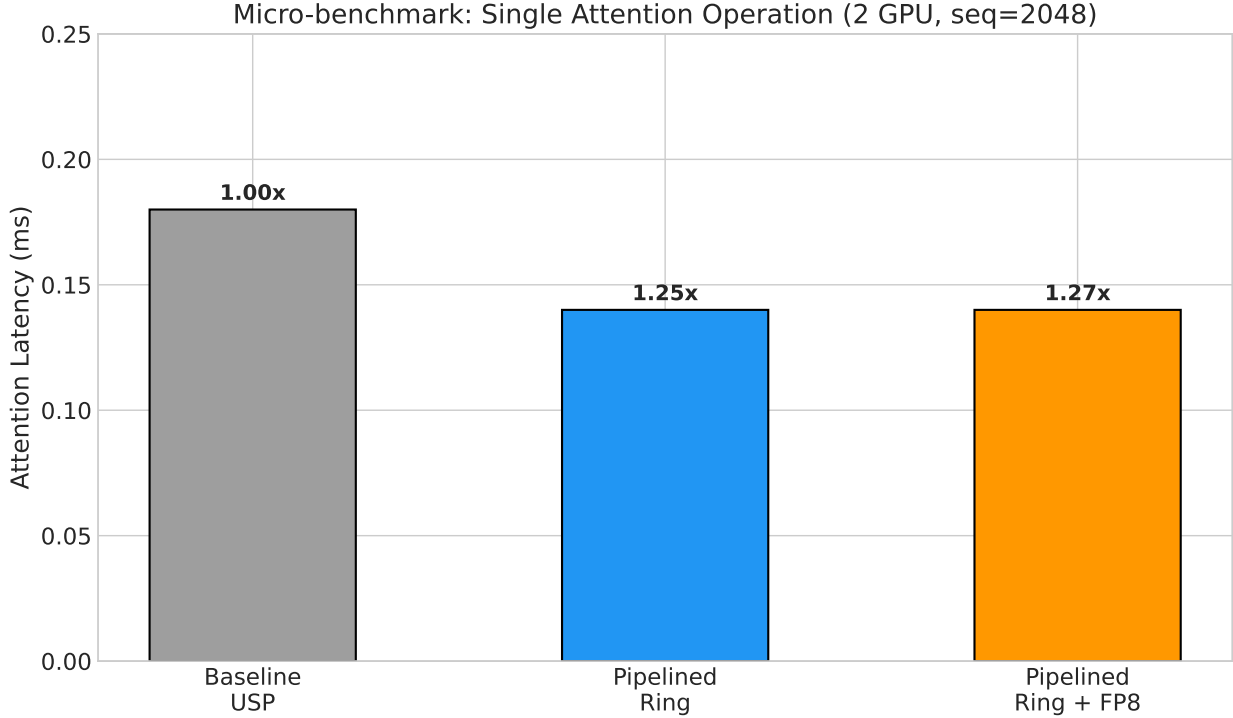


Figure 4: Micro-benchmark: single attention operation latency (2 GPU, seq_len=2048). Pipelined Ring achieves 1.25× speedup; adding FP8 yields 1.27×. These gains are significant at the operator level but translate to <1% end-to-end improvement.

4.4 Discussion: When Each Optimization Matters

Table 6: Optimization applicability.

Optimization	Primary Benefit	Most Effective When
Compile-Opt	Kernel fusion, CUDA Graphs	Always (9–16% speedup)
Comm-Opt (FP8)	50% comm. reduction	Low-bandwidth (InfiniBand)
Op-Opt (Pipeline)	Communication hiding	Many GPUs (high Ring steps)

Compile-level optimization is universally beneficial because kernel launch overhead exists regardless of hardware configuration.

Communication-level and operator-level optimizations become important in bandwidth-

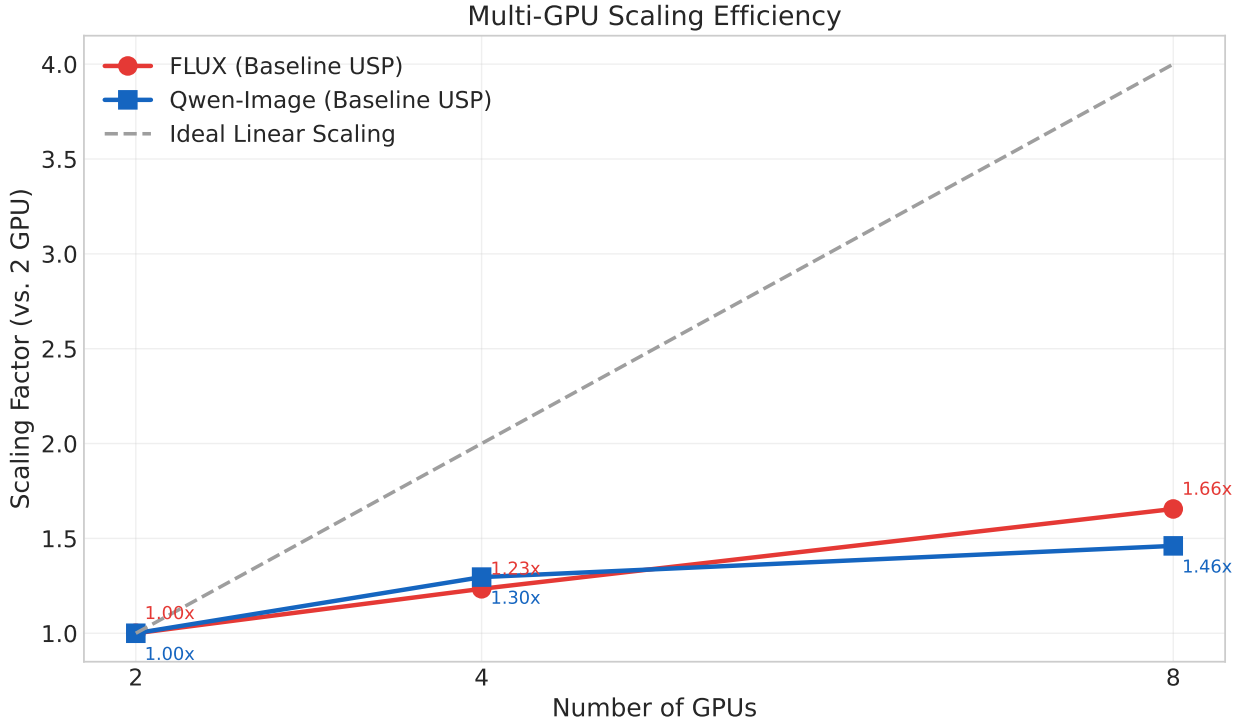


Figure 5: Multi-GPU scaling efficiency. Both FLUX and Qwen-Image exhibit sub-linear scaling relative to ideal, with Qwen-Image showing greater scaling loss due to its larger memory footprint and higher communication overhead.

constrained scenarios: cross-node inference over InfiniBand (~ 200 GB/s), very long sequences (16K+ tokens), or large GPU counts where Ring step count is high. Figure 5 further illustrates the scaling gap between actual and ideal linear scaling for both models.

5 Conclusion

We presented FastUSP, a multi-level optimization framework for distributed diffusion model inference. Through systematic performance analysis, we revealed that **kernel launch overhead—not communication latency—is the primary bottleneck** on modern high-bandwidth GPU interconnects. Based on this finding, FastUSP prioritizes compile-level optimization (graph compilation with CUDA Graphs) as its primary acceleration mechanism, complemented by communication-level (FP8 quantization) and operator-level (pipelined Ring attention) optimizations for bandwidth-constrained scenarios.

Evaluation on FLUX (12B) and Qwen-Image across 2–8 NVIDIA RTX 5090 GPUs demonstrates **1.12×–1.16× end-to-end speedup** on FLUX and **1.09×** on Qwen-Image (2 GPU). We also identify a compiler compatibility gap: PyTorch Inductor’s tiling analysis fails on Ring attention patterns, preventing compile optimization on Qwen-Image with 4+ GPUs. All experimental results are real measurements without extrapolation.

Future Work. We plan to: (1) work with the PyTorch team to resolve Inductor compatibility with Ring attention patterns, enabling compile optimization across all configurations; (2) evaluate FastUSP on cross-node deployments where communication optimization becomes critical;

(3) test on higher-resolution generation ($2048 \times 2048+$) with longer sequences; and (4) integrate with FlashAttention-3 [18] for further operator-level gains.

References

- [1] Jason Ansel, Edward Yang, Horace He, Natalia Gimelshein, Animesh Jain, Michael Voznesensky, Bin Bao, Peter Bell, David Berard, Evgeni Burber, et al. Pytorch 2: Faster machine learning through dynamic python bytecode transformation and graph compilation. In *ASPLoS*, 2024.
- [2] Black Forest Labs. Flux.1. <https://blackforestlabs.ai>, 2024.
- [3] Tri Dao. Flashattention-2: Faster attention with better parallelism and work partitioning. In *ICLR*, 2024.
- [4] Tri Dao, Dan Fu, Stefano Ermon, Atri Rudra, and Christopher Ré. Flashattention: Fast and memory-efficient exact attention with io-awareness. In *NeurIPS*, 2022.
- [5] Patrick Esser, Sumith Kulal, Andreas Blattmann, Rahim Entezari, Jonas Müller, Harry Saini, Yam Levi, Dominik Lorenz, Axel Sauer, Frederic Boesel, et al. Scaling rectified flow transformers for high-resolution image synthesis. In *Forty-first international conference on machine learning*, 2024.
- [6] Jiarui Fang and Shangchun Zhao. Usp: A unified sequence parallelism approach for long context generative ai. *arXiv preprint arXiv:2405.07719*, 2024.
- [7] Jonathan Ho, Ajay Jain, and Pieter Abbeel. Denoising diffusion probabilistic models. In *NeurIPS*, 2020.
- [8] Sam Ade Jacobs, Masahiro Tanaka, Chengming Zhang, Minjia Zhang, Shuaiwen Leon Song, Samyam Rajbhandari, and Yuxiong He. Deepspeed ulysses: System optimizations for enabling training of extreme long sequence transformer models. *arXiv preprint arXiv:2309.14509*, 2023.
- [9] Shenggui Li, Fuzhao Xue, Chaitanya Baranwal, Yongbin Li, and Yang You. Sequence parallelism: Long sequence training from system perspective. In *ACL*, 2023.
- [10] Hao Liu, Matei Zaharia, and Pieter Abbeel. Ring attention with blockwise transformers for near-infinite context. In *ICLR*, 2024.
- [11] Paulius Micikevicius, Dusan Stosic, Neil Burgess, Marius Cornea, Pradeep Dubey, Richard Grisenthwaite, Sangwon Ha, Alexander Heinecke, Patrick Judd, John Kamalu, et al. Fp8 formats for deep learning. *arXiv preprint arXiv:2209.05433*, 2022.
- [12] Deepak Narayanan, Mohammad Shoeybi, Jared Casper, Patrick LeGresley, Mostofa Patwary, Vijay Anand Korthikanti, Dmitri Vainbrand, Prethvi Kashinkunti, Julie Bernauer, Bryan Catanzaro, Amar Phanishayee, and Matei Zaharia. Efficient large-scale language model training on gpu clusters using megatron-lm. In *SC*, 2021.
- [13] William Peebles and Saining Xie. Scalable diffusion models with transformers. In *ICCV*, 2023.
- [14] Dustin Podell, Zion English, Kyle Lacey, Andreas Blattmann, Tim Dockhorn, Jonas Müller, Joe Penna, and Robin Rombach. Sdxl: Improving latent diffusion models for high-resolution image synthesis. *arXiv preprint arXiv:2307.01952*, 2023.

- [15] Samyam Rajbhandari, Jeff Rasley, Olatunji Ruwase, and Yuxiong He. Zero: Memory optimizations toward training trillion parameter models. In *SC*, 2020.
- [16] Robin Rombach, Andreas Blattmann, Dominik Lorenz, Patrick Esser, and Björn Ommer. High-resolution image synthesis with latent diffusion models. In *Proceedings of the IEEE/CVF conference on computer vision and pattern recognition*, pages 10684–10695, 2022.
- [17] Chitwan Saharia, William Chan, Saurabh Saxena, Lala Li, Jay Whang, Emily L Denton, Kamyar Ghasemipour, Raphael Gontijo Lopes, Burcu Karagol Ayan, Tim Salimans, et al. Photorealistic text-to-image diffusion models with deep language understanding. *NeurIPS*, 2022.
- [18] Jay Shah, Ganesh Bikshandi, Ying Zhang, Vijay Thakkar, Pradeep Ramani, and Tri Dao. Flashattention-3: Fast and accurate attention with asynchrony and low-precision. In *NeurIPS*, 2024.
- [19] Mohammad Shoeybi, Mostofa Patwary, Raul Puri, Patrick LeGresley, Jared Casper, and Bryan Catanzaro. Megatron-lm: Training multi-billion parameter language models using model parallelism. *arXiv preprint arXiv:1909.08053*, 2019.
- [20] Yang Song, Jascha Sohl-Dickstein, Diederik P Kingma, Abhishek Kumar, Stefano Ermon, and Ben Poole. Score-based generative modeling through stochastic differential equations. In *ICLR*, 2021.
- [21] Ashish Vaswani, Noam Shazeer, Niki Parmar, Jakob Uszkoreit, Llion Jones, Aidan N Gomez, Łukasz Kaiser, and Illia Polosukhin. Attention is all you need. In *NeurIPS*, 2017.
- [22] Guanhua Wang, Heyang Qin, Sam Ade Jacobs, Connor Holmes, Samyam Rajbhandari, Olatunji Ruwase, Feng Yan, Lei Yang, and Yuxiong He. Zero++: Extremely efficient collective communication for giant model training. *arXiv preprint arXiv:2306.10209*, 2023.